第 32 卷第 6 期 无 机 化 学 学 报 Vol.32 No.6
2016 年 6 月 CHINESE JOURNAL OF INORGANIC CHEMISTRY 1063-1070

表面稳定单质铜的介孔二氧化钛的光催化产氢性能

刘娟娟 乔培胜 过军芳 邹世辉 肖丽萍* 范 杰*
(浙江大学化学系,杭州 310027)

摘要:采用十二烷基硫醇作为保护剂有效地稳定住了光催化过程中介孔二氧化钛(m-TiO_2)表面原位生成的 Cu^0 物种。通过 X 射线衍射,X 射线光电子能谱,高分辨透射电镜,高角环形暗场扫描透射电镜等手段对催化剂的组成结构进行了表征,发现催化剂中仅有 Cu^0 物种存在。在紫外光照射下,以甲醛水溶液为牺牲试剂测试了 Cu^0 物种对介孔二氧化钛产氢性能的影响,发现适量的 Cu^0 纳米颗粒能够极大地提高介孔二氧化钛的产氢性能。当 Cu^0 的物质的量分数为 1.0%时,Cu^0/m-TiO_2 表现出最高的产氢速率,为 725 $\mu mol \cdot h^{-1} \cdot g^{-1}$。该样品中 Cu^0 纳米颗粒的尺寸为(4.2±0.9) nm。此外,通过气相色谱检测到产生的 H_2 和 CO_2 的物质的量之比为 2:1,表明部分氢气来自于水分解。

关键词:单质铜;介孔二氧化钛;光催化产氢;甲醛
中图分类号:O643.3;O614.41+1;O614.121 **文献标识码**:A **文章编号**:1001-4861(2016)06-1063-08
DOI:10.11862/CJIC.2016.143

Stabilizing Metallic Cu^0 on the Surface of m-TiO_2 for Photocatalytic H_2 Production

LIU Juan-Juan QIAO Pei-Sheng GUO Jun-Fang ZOU Shi-Hui XIAO Li-Ping* FAN Jie*
(*Department of Chemistry, Zhejiang University, Hangzhou, Zhejiang* 310027, *China*)

Abstract: Dodecanethiol was introduced as a protective agent to stabilize the *in situ* generated Cu^0 species on the surface of mesoporous TiO_2 (m-TiO_2). The as-produced samples were characterized by XRD, XPS, HRTEM and HADDF-STEM. It is noteworthy that only Cu^0 species were detected in these samples. The system thus served as an excellent model to investigate Cu^0-incorporated m-TiO_2. Photocatalytic measurements suggested that the Cu^0 species could greatly enhance the photocatalytic H_2-evolution activity of m-TiO_2 in formaldehyde solution. Moreover, we found that the activity depends on the concentration of Cu^0. The maximum H_2 evolution rate of 725 $\mu mol \cdot h^{-1} \cdot g^{-1}$ is obtained on 1.0% Cu/m-TiO_2, with average Cu^0 particle size of (4.2±0.9) nm. It is interesting to find that in our case, the molar ratio of produced H_2 to CO_2 is 2:1, which indicates the involvement of H_2O as hydrogen source.

Keywords: Cu^0 species; mesoporous TiO_2; photocatalytic H_2 evolution; formaldehyde

Hydrogen (H_2) has been considered as a promising fuel candidate of next generation in industries due to its high energy capacity (142 $MJ \cdot kg^{-1}$), environmental friendliness and recycling possibility[1-6]. Currently, H_2 is mainly produced by steam reforming of fossil, which is accompanied with the emission of harmful gases (NO_x or SO_2) and particulate matters[7-9]. From a clean-energy perspective, fabricating emission-free pathway to produce hydrogen is important for applications of "hydrogen economy", which drive people's attention to water splitting, especially semiconductor-based photocatalytic hydrogen production[10-12].

收稿日期:2016-03-03。收修改稿日期:2016-03-26。
国家自然科学基金(No.21271153,21373181,21222307,U1402233),国家自然科学基金重大研究计划(No.91545113)资助项目。
*通信联系人。E-mail:lpxiao@zju.edu.cn,jfan@zju.edu.cn;会员登记号:S06N4298S1406。

Over the past 40 years, a large number of semiconductors have been developed as photocatalysts to split water into H_2 and O_2[13-20]. Among them, TiO_2 is the most investigated due to its low cost, high chemical stability, excellent photostability and environmental-friendly characters[21-26]. However, the H_2 evolution efficiency of photocatalytic water splitting over bare TiO_2 remains quite limited because of the fast recombination of photogenerated electron/hole pairs as well as the rapid backward reaction between hydrogen and oxygen[27-29]. To overcome these shortcomings, extensive efforts have been devoted to develop modification techniques of TiO_2, including noble metal loading, heteroelement doping, sacrificial reagents addition, dye sensitization and so on[30-35]. From a cost efficiency perspective, it is of great interest to fabricate transition metal modified TiO_2 with organic wastes (formaldehyde, glycerol *etc*.) as sacrificial reagents to produce H_2[36-38].

It was shown that Cu-incorporated TiO_2 are efficient in photocatalytic H_2 production[39-41]. Conventionally, the majority studies are focused on CuO or Cu_2O modified TiO_2. For example, Bandara et al. fabricated a highly stable CuO deposited TiO_2 photocatalyst and found that CuO could promote the charge separation and act as a water reduction site[39]. Yu and coworkers investigated the possibility of using CuO and Cu $(OH)_2$ cluster as effective co-catalyst to enhance the photocatalytic H_2-production activity of TiO_2[5,42]. A quantum size effect of CuO cluster was observed to alter the energy levels of conduction and valence band edges in the CuO-TiO_2 semiconductor systems while the formation of Cu clusters was believed to facilitate the electron transfer from the conductive band (CB) of TiO_2 to Cu $(OH)_2$ and the reduction of H^+[11]. On the other hand, Wu et al. fabricated different CuO_x species over TiO_2 and discovered that Cu^+ species could promote photocurrent generation while Cu^{2+} species inhibits the activity[43]. Considering all these aforementioned studies, the actual functions of different Cu species, especially Cu^0 are still unclear since Cu^0 is easily oxidized in air[44]. This in return motivates us to develop techniques to stabilize the metastable state (Cu^0 and Cu^+) of Cu species.

In this study, we introduced dodecanethiol (DDT) as a protective agent to stabilize the *in situ* generated Cu^0 species on the surface of *m*-TiO_2. DDT was chosen because it could form self-assembled monolayers around Cu species but does not change Cu species chemical state[45]. Catalytic measurements showed that Cu^0-incoporated *m*-TiO_2 exhibited much better H_2-evolution performance than bare *m*-TiO_2. The molar ratio of produced H_2 and CO_2 was determined to be 2∶1, indicating the involvement of H_2O as hydrogen source. Besides, we found that H_2 production activities were strongly dependent on the concentration of Cu^0. The maximum H_2-evolution rate of 725 $\mu mol \cdot h^{-1} \cdot g^{-1}$ was obtained on 1.0% Cu/*m*-TiO_2, with average particle size of 4.2±0.9 nm.

1 Experimental

1.1 Synthesis of *m*-TiO_2

All the chemical reagents used in this study were of analytical grade and were used without further purification. *m*-TiO_2 was synthesized via a sol-gel process according to reported literatures with some modifications[46]. In a typical synthesis, 10 mmol of $Ti(OBu)_4$, 40 mmol HOAc, 12 mmol HCl, and 1.6 g of F127 ($EO_{96}PO_{70}EO_{96}$, M_r=12 000) were dissolved in 30 mL of ethanol. The mixture was stirred vigorously for 1 h to obtain a clear solution and then the solution was transferred into a petri dish (i.d. =125 mm). The ethanol was evaporated at 40 ℃ with a relative humidity of 30%~80%. After the solvent was evaporated, it was transferred into a 65 ℃ oven and aged for 24 h. The as-synthesized mesostructured hybrids were calcined at 350 ℃ in air for 6 h (ramp rate 2 ℃·min^{-1}) to obtain *m*-TiO_2.

1.2 C_xT catalysts preparation and photocatalytic test of H_2 production

C_xT catalysts preparation and photocatalytic H_2 evolution experiments were carried out at 25 ℃ under light irradiation by a 300 W high-pressure Hg lamp. In a typical reaction system, 40 mg of *m*-TiO_2 and a certain amount of $CuCl_2$ aqueous solution (0.05 mol·L^{-1}) were mixed into 10 mL of formaldehyde solution (2%), and then the oxygen was completely eliminated

by Ar. The reaction tube was sealed in absence of air. The amount of produced H_2 and CO_2 was monitored by GC-TCD. After photocatalysis, 200 μL of DDT was injected into the reaction mixture. The solid was collected after 10 min vigorous stirring by centrifugation, washed twice with water and ethanol. Then, the solid was dried in a vacuum oven at 30 ℃ overnight. The samples were labeled as C_xT, where x is the molar ratio of Cu to Ti (x=0.1, 0.5, 1.0, 5.0, 10.0).

1.3 Characterization

The small-angle X-ray scattering (SAXS) patterns were collected on a Nanostar U SAXS system (Germany) using Cu $K\alpha$ radiation at 40 kV and 35 mA to determine structural quality and symmetry. Nitrogen adsorption isotherms were measured at −196 ℃ on a Micromeritics ASAP 2020 adsorption analyzer. Wide-angle X-ray diffraction (XRD) patterns were recorded on a Rigaku Ultimate Ⅳ operated at 40 mA and 40 kV with Cu $K\alpha$ radiation (λ=0.154 178 nm) at a scan rate of 5°·min^{-1}. XPS measurements were performed on a VG Scientific ESCALAB Mark Ⅱ spectrometer equipped with two ultra-high vacuum (UHV) chambers. All binding energies were referenced to the C1s peak at 284.8 eV of the surface adventitious carbon. High resolution transmission electron microscopy (HRTEM) images, HADDF-STEM and EDS measurements were recorded on a TECNAI G2 F20 operated at 200 kV.

2 Results and discussion

2.1 Characterization of materials

Fig.1a shows the SAXS pattern of the as-produced TiO_2. The well-resolved diffraction peaks can be indexed to the (100) reflections of a two-dimensional hexagonal phase with an interplanar distance of 10.0 nm, indicating an ordered mesoporous structure of TiO_2[47]. The conclusion is further confirmed by N_2 sorption isotherms of TiO_2 which show a type-Ⅳ curve with a clear capillary condensation step (Fig.1b)[48]. The pore size of the produced TiO_2 is *ca.* 4.2 nm and the surface area of TiO_2 is as high as 220.2 m^2·g^{-1}. In addition, the typical mesoporous structure can be seen from TEM images (Fig.1a inset) as well.

XRD measurements were carried out to determine the phase structure and crystalline size of the collected samples. As can be seen from Fig.2, no characteristic diffraction peaks of Cu species were detected when the $CuCl_2$ loading content is lower than 1.0%, implying the small particle size and good dispersion of Cu species. In contrast, once the Cu content is higher than 5.0%, two sharp peaks at 43.4° and 55.6° were observed, corresponding to (111) and

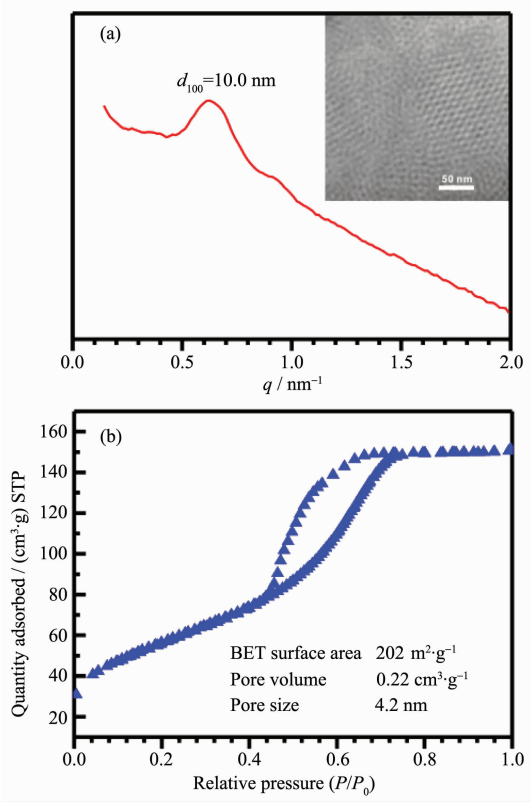

Fig.1 (a) SAXS (inset: TEM) data and (b) N_2 adsorption-desorption isotherms of m-TiO_2

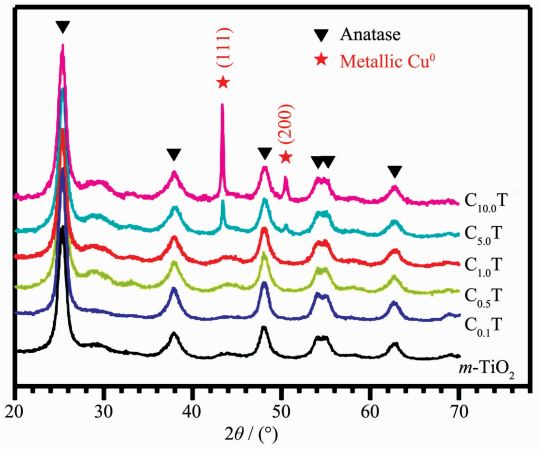

Fig.2 XRD patterns of m-TiO_2 and C_xT (x=0.1, 0.5, 1.0, 5.0 and 10.0)

(200) of Cu^0 (JCPDS 65-9743), respectively[49-50]. The crystalline sizes of Cu^0 particles in $C_{5.0}T$ and $C_{10.0}T$ were calculated to be *ca.* 27.4 nm and 39.7 nm by Scherrer formula, respectively, indicating that the sizes of Cu^0 particles are closely related to the Cu content. On the other hand, all samples exhibited similar XRD peaks for anatase without evident shifts, implying that there was no significant change in crystalline structure of *m*-TiO_2. And the deposited Cu^0 mainly attached on the surface of *m*-TiO_2 rather than incorporated into the lattice of *m*-TiO_2.

The chemical states of Cu species in C_xT were further verified by XPS measurements. As shown in Fig.3, two symmetrical peaks at *ca.* 932.4 and 952.3 eV were observed for all samples, which could be attributed to the dominant $Cu^0 2p_{3/2}$ and $Cu^0 2p_{1/2}$, respectively[51-52]. No other peaks belonging to Cu species (Cu^+ or Cu^{2+}) were detected, indicating a completely conversion from Cu^{2+} to Cu^0. Notably, in the absence of DDT, all Cu species (Cu^0, Cu^+ and Cu^{2+}) were detected, confirming the instability of Cu^0 in air. These results, on the other hand, verify the feasibility of utilizing DDT to stabilize Cu^0. Besides, Ti2*p* peaks were in good agreement with those of Ti^{4+} reported in literatures[53]. The system can thus serve as a model system to investigate the effect of Cu^0 as co-catalyst of *m*-TiO_2.

The microstructures of C_xT were further investigated by STEM, HRTEM and EDX analysis. EDX analyses (Fig.4b and 4e) display that the typical brighter spots in cycles in Fig.4a and Fig.4d are Cu species, while the background circles mainly consist of TiO_2 support. The lattice fringe of typical Cu nanoparticle (Fig.4c) displays inter-planar spacing of 0.209 nm, which matches well with the (111) plane of Cu^0 species[54]. STEM images shown in Fig.4a demonstrate that the Cu^0 nanoparticles in $C_{1.0}T$ catalyst are well dispersed on the *m*-TiO_2 framework. The sizes of the Cu^0 particles are rather small with a narrow size distribution ((4.2 ±0.9) nm). Compared with $C_{1.0}T$ sample, the size of Cu^0 particle in $C_{10.0}T$ catalyst is much bigger with an average of (38.4±5.2) nm (Fig.4d and 4f). These results coincide with the XRD results, again confirming that the Cu^0 particle sizes are determined by the Cu content.

The conclusion is also confirmed by the UV-Vis spectra. As can be seen in Fig.5, there is no remarkable difference between *m*-TiO_2 and C_xT in the UV-absorption region (*i.e.* 300~400 nm), suggesting they have similar band structures. Nevertheless, C_xT samples display broad peaks in the range of 500~800 nm with the intensities increasing along with the Cu^0 loading amount. These results, in line with the HRTEM data and literature results[55-57], indicate that the Cu^0 particle size is increased due to the increased loading amount.

2.2 Photocatalytic H_2 evolution from HCHO/H_2O

Photocatalytic activities of various samples were evaluated under UV-irradiation using formaldehyde as a sacrificial agent. We chose this reaction because it

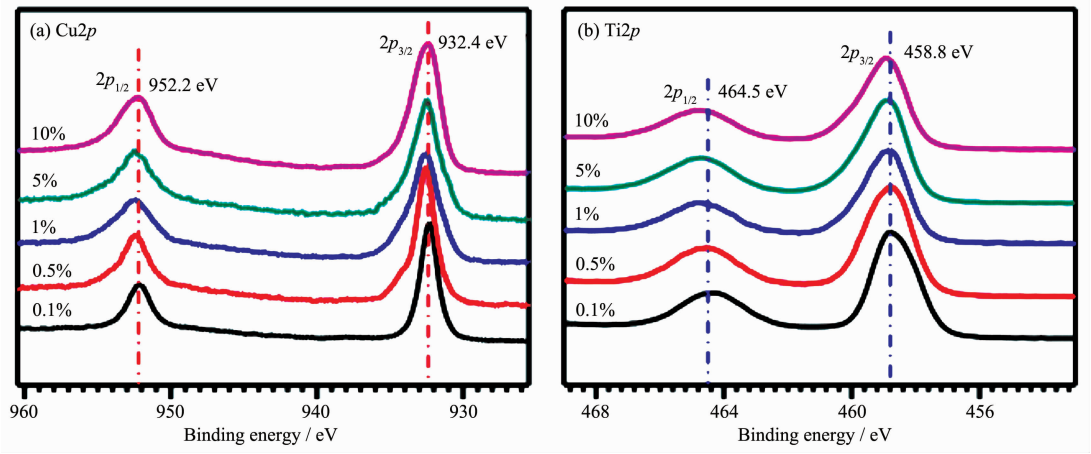

Fig.3 XPS spectra of C_xT (x=0.1, 0.5, 1.0, 5.0, 10.0)

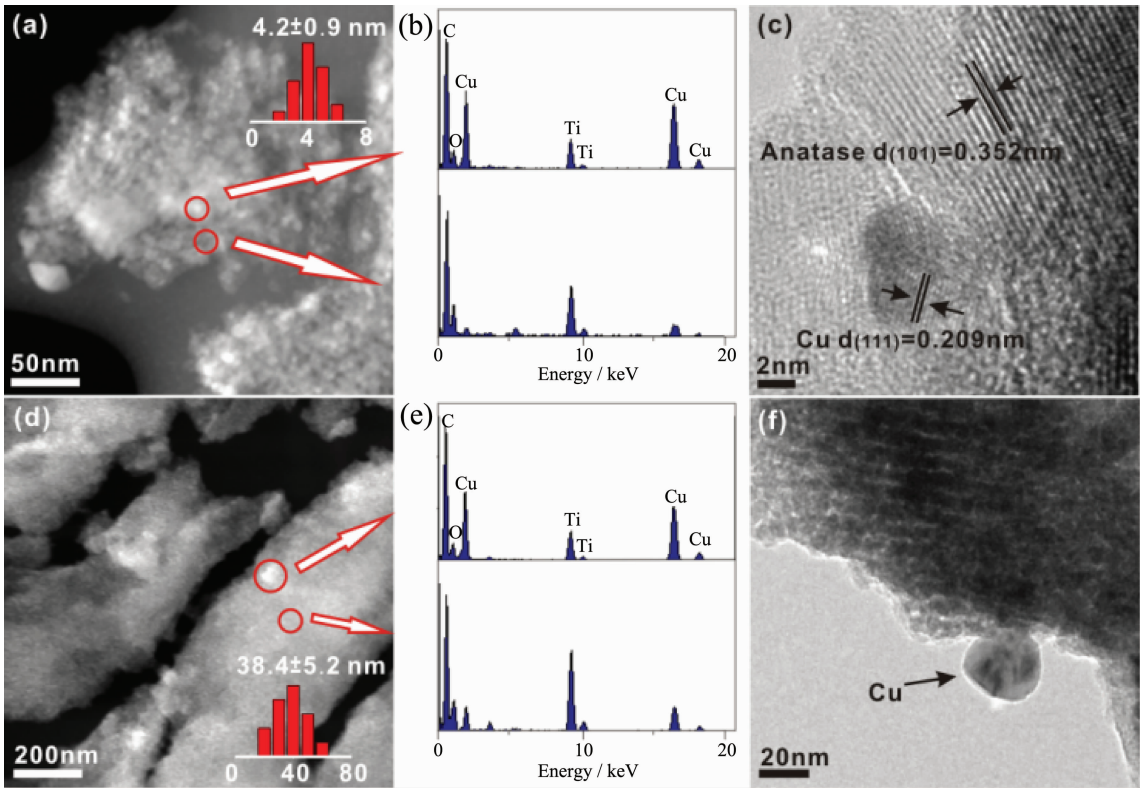

Fig.4　HAADF-STEM images, EDX analysis, HR-TEM images of (a)~(c) $C_{1.0}T$ and (d)~(f) $C_{10.0}T$

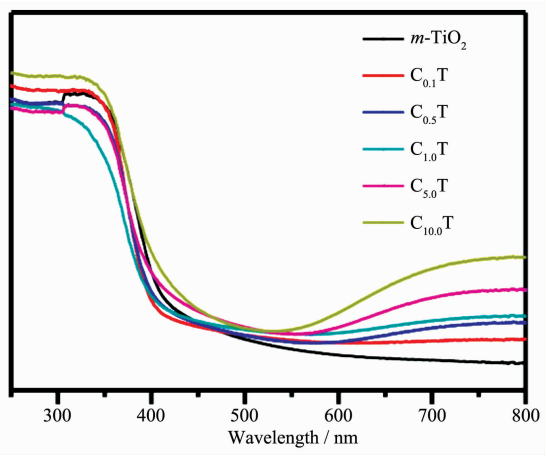

Fig.5　UV-Vis spectra of the C_xT catalysts

is an efficient and low-cost procedure which combines the abatement of organic wastewater pollutants with energy generation. Control experiments indicated that no appreciable hydrogen production was detected in the absence of either irradiation or photocatalyst, suggesting that hydrogen was produced by photocatalytic reactions on catalyst. Fig.6 shows a comparison of the photocatalytic performance on various samples. As can be seen in this figure, all of the C_xT (x=0.1, 0.5, 1.0, 5.0, 10.0) catalysts exhibit superior activities than pure m-TiO_2, suggesting that Cu^0 could significantly enhance the photocatalytic H_2-production activity of m-TiO_2. Interestingly, the activities are also related to the Cu content. When the Cu content in C_xT is lower than 1.0% ($C_{0.1}T$, $C_{0.5}T$ and $C_{1.0}T$), the H_2-evolution rate increases along with the Cu content. It is important to highlight that with a small amount of $CuCl_2$ addition ($C_{0.1}T$), the H_2 production is significantly improved from *ca.* 16 μmol to 400 μmol. The highest photocatalytic H_2 evolution rate, 725 $\mu mol \cdot g^{-1} \cdot h^{-1}$, is obtained on $C_{1.0}T$, which is *ca.* 10 times higher than that of bare m-TiO_2. To further increase the $CuCl_2$ loading content to 5.0% and 10.0% ($C_{5.0}T$ and $C_{10.0}T$), a decrease in the H_2 evolution rate is observed. Especially, there is a drastic decrease in the H_2 production on $C_{10.0}T$ sample. It is interesting to find that the variation of H_2-evolution rate to Cu content is similar to that of the Cu^0 particle size. The drastic decrease in the H_2 production on $C_{10.0}T$ is likely due to the significantly increased Cu^0 size, which is unfavorable for charge transfer.

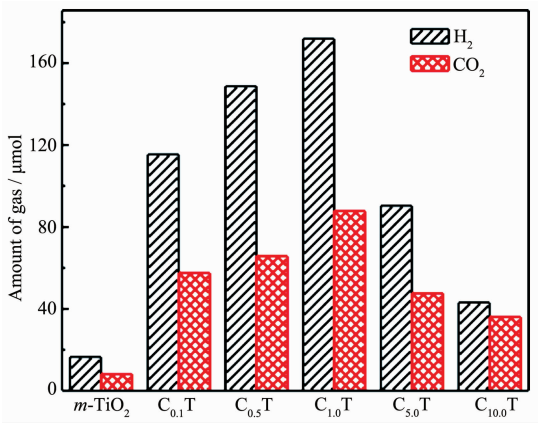

Fig.6 Amount of H_2 and CO_2 produced by C_xT within 6 h under UV-irradiation

On the other hand, we find that for all samples except $C_{10.0}T$, the molar ratio of the produced H_2 and CO_2 is *ca.* 2:1. Given that there are only two H atoms within a HCHO molecule, the H_2/CO_2 molar ratio of 2:1 indicates that H_2O is involved in the reaction. The overall reaction equation is then:

$$HCHO+H_2O \longrightarrow 2H_2+CO_2$$

The H_2/CO_2 molar ratio of $C_{10.0}T$ is less than 2:1 because certain amount of CO_2 is produced during the reduction of Cu^{2+} to Cu^0. As shown in Fig.7, at the beginning of reaction, more CO_2 is produced than H_2 on $C_{10.0}T$.

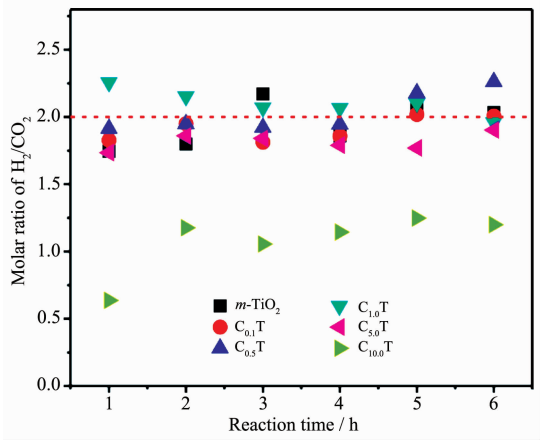

Fig.7 Time course of H_2/CO_2 molar ratio for C_xT

To better understand the catalytic mechanisms, as well as to further verify the function of Cu^0 as co-catalyst for *m*-TiO_2, the anion effect with equal molar ratio of Cu species was investigated. As can be seen in Fig.8, there is only a tiny difference between the varied Cu salts for H_2 evolution rates, with the order of $CuCl_2>Cu(Ac)_2>CuSO_4>Cu(NO_3)_2$, suggesting that the Cu^0 species rather than Cl^- are the main active species to enhance the activity of m-TiO_2. Combining the results in Fig.6, we can safely conclude that Cu^0 species play a decisive role in photocatalytic H_2 evolution.

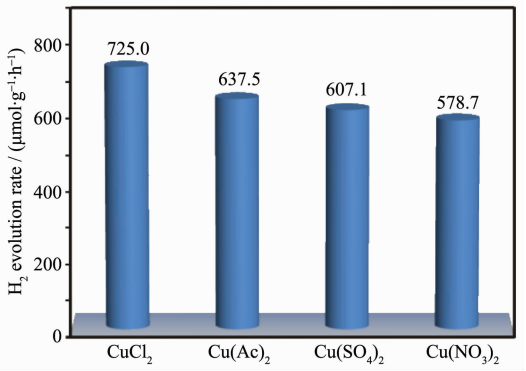

Fig.8 H_2 evolution rates of m-TiO_2 with various Cu salts (molar ratio of Cu to Ti is fixed at 1.0%)

On the other hand, the promoting effect of Cu^0 is not limited to *m*-TiO_2. As shown in Fig.9, the addition of 1.0% $CuCl_2$ salt in ZnO, WO_3 and P25 systems can also significantly improve the H_2-evolution rate. The sequences of H_2-evolution rates is P25 >ZnO >WO_3, largely in agreement with the capability of semiconductors in producing electron/hole pairs under UV irradiation. In addition, we also found that the structural variation can regulate the catalytic performance. It shows the activity on *m*-TiO_2 is much higher than that on P25 (TiO_2 particles). This difference mainly results from the higher surface areas (50 $m^2 \cdot g^{-1}$ vs 220 $m^2 \cdot g^{-1}$ for P25 vs *m*-TiO_2, respectively) and easier mass diffusion/adsorption on ordered mesoporous TiO_2.

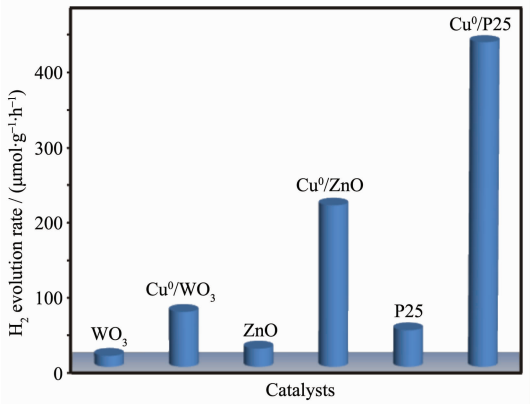

Fig.9 H_2 evolution rates (within 6 h) of WO_3, ZnO, P25 with and without 1.0% $CuCl_2$

Based on above evidences, the mechanism of photocatalytic H_2 evolution in formaldehyde solution over Cu^0/m-TiO_2 is illustrated in Scheme 1. Under UV irradiation, Cu^{2+} species is quickly reduced to Cu^0 species, which is the main factor responsible for photocatalytic H_2 evolution improvement. The promotion effect is similar with noble metal supported on TiO_2, such as Au or Pt[58-59]. In current system, the electron/hole recombination is decreased due to the presence of Cu^0 nanoparticles, which could capture the electrons and reduce HCHO and H_2O to H_2. On the other hand, the organic sacrificial molecules (formaldehyde) can combine with the holes, and then be oxidized into CO_2. The reduced electron/hole recombination improves the utilization efficiency of excited electrons and thus results in an enhanced H_2-evolution performance.

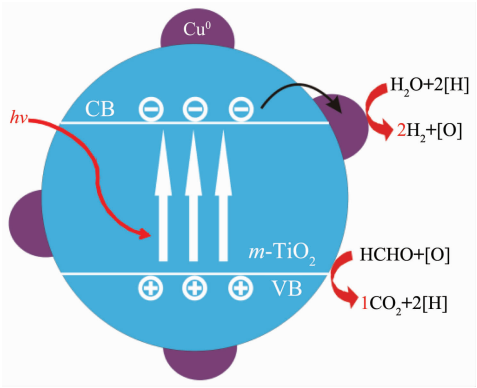

Scheme 1　Schematic illustration for the charge transfer on C_xT in photocatalytic H_2 evolution

Moreover, there exists a particle size effect of metallic Cu^0 in photocatalytic H_2 evolution in formaldehyde solution. For $C_{1.0}T$ samples, sub-5 nm Cu^0 nanoparticles are uniformly distributed on m-TiO_2, which facilitates the electron transfer from m-TiO_2 to Cu^0 and subsequently HCHO and H_2O can be reduced to H_2. By comparison, $C_{10.0}T$ sample with high $CuCl_2$ content forms large Cu nanoparticles, which is unfavorable for charge transfer. This is similar with the size-dependent photocatalytic properties of Au nanoparticles deposited on TiO_2[59]. The photocatalysis activity can be decreased with the growing bigger particles.

3　Conclusions

In summary, we successfully stabilized the in situ generated Cu^0 species by DDT. Characterizations on the samples suggested the only presence of Cu^0 species, which make this system a perfect model to investigate the function of Cu^0 as co-catalyst for m-TiO_2. Photocatalytic measurements showed that Cu^0 could greatly improve the H_2-evolution rate of m-TiO_2. The molar ratio of H_2/CO_2 on Cu^0/m-TiO_2 is 2:1, indicating the involvement of H_2O as hydrogen source. Besides, we found that the H_2-evolution rate also depends on the particle size of Cu^0. The sub-5 nm Cu^0 nanoparticles favor the charge transfer and thus improve the H_2 evolution. Our study clarifies the function of Cu^0 as co-catalyst for m-TiO_2, which may provide valuable insights into a detailed understanding of the whole Cu-incorporated TiO_2 systems in photocatalysis.

Acknowledgements: We are grateful to Department of Chemistry and Department of Materials in Zhejiang University for XPS and TEM measurements.

References:

[1] Walter M G, Warren E L, McKone J R, et al. *Chem. Rev.*, **2010**,**110**(11):6446-6473

[2] Bi Q Y, Du X L, Liu Y M, et al. *J. Am. Chem. Soc.*, **2012**, **134**(21):8926-8933

[3] Chen X, Shen S, Guo L, et al. *Chem. Rev.*, **2010**,**110**(11): 6503-6570

[4] Yamada Y, Yano K, Xu Q, et al. *J. Phys. Chem. C*, **2010**, **114**(39):16456-16462

[5] Yu J, Hai Y, Jaroniec M. *J. Colloid Interface Sci.*, **2011**,**357** (1):223-228

[6] Zong X, Yan H, Wu G, et al. *J. Am. Chem. Soc.*, **2008**,**130** (23):7176-7177

[7] Bulut A, Yurderi M, Karatas Y, et al. *ACS Catal.*, **2015**,**5** (10):6099-6110

[8] Peng B, Chen J. *Energy Environ. Sci.*, **2008**,**1**(4):479-483

[9] Yamada Y, Yano K, Fukuzumi S. *Energy Environ. Sci.*, **2012**,**5**(1):5356-5363

[10]Kudo A, Miseki Y. *Chem. Soc. Rev.*, **2009**,**38**(1):253-278

[11]Maeda K, Domen K. *J. Phys. Chem. Lett.*, **2010**,**1**(18):2655-2661

[12]Osterloh F E. *Chem. Mater.*, **2008**,**20**(1):35-54

[13]Fujishima A. *Nature*, **1972**,**238**:37-38

[14]Choi W, Termin A, Hoffmann M R. *J. Phys. Chem.*, **1994**,**98**(51):13669-13679

[15]Asahi R, Morikawa T, Ohwaki T, et al. *Science*, **2001**,**293**(5528):269-271

[16]Yu J C, Yu J, Ho W, et al. *Chem. Mater.*, **2002**,**14**(9):3808-3816

[17]Sakthivel S, Kisch H. *Angew. Chem., Int. Ed.*, **2003**,**42**(40):4908-4911

[18]Tsuji I, Kato H, Kobayashi H, et al. *J. Am. Chem. Soc.*, **2004**,**126**(41):13406-13413

[19]Maeda K, Teramura K, Lu D, et al. *Angew. Chem.*, **2006**,**118**(46):7970-7973

[20]Wang H, Zhang L, Chen Z, et al. *Chem. Soc. Rev.*, **2014**,**43**(15):5234-5244

[21]Kamat P V. *J. Phys. Chem. C*, **2007**,**111**(7):2834-2860

[22]Priebe J B, Karnahl M, Junge H, et al. *Angew. Chem., Int. Ed.*, **2013**,**52**(43):11420-11424

[23]Zhou M, Yu J, Liu S, et al. *Appl. Catal. B*: *Environ.*, **2009**, **89**(1/2):160-166

[24]YANG Juan(杨娟), LI Jian-Tong(李建通), MIU Juan(缪娟). *Chinese J. Inorg. Chem.*(无机化学学报), **2011**,**27**(3):547-555

[25]LI Fang-Bo(李芳柏), GU Guo-Bang(古国榜), LI Xin-Jun(李新军), et al. *Chinese J. Inorg. Chem.*(无机化学学报), **2001**, **17**(1):37-42

[26]REN Ling(任凌), YANG Fa-Da(杨发达), ZHANG Yuan-Ming(张渊明), et al. *Chinese J. Inorg. Chem.*(无机化学学报), **2008**,**24**(4):541-546

[27]Xu S, Sun D D. *Int. J. Hydrogen Energy*, **2009**,**34**(15):6096-6104

[28]Tachikawa T, Fujitsuka M, Majima T. *J. Phys. Chem. C*, **2007**,**111**(14):5259-5275

[29]Cermenati L, Pichat P, Guillard C, et al. *J. Phys. Chem. B*, **1997**,**101**(14):2650-2658

[30]Xin B, Jing L, Ren Z, et al. *J. Phys. Chem. B*, **2005**,**109**(7):2805-2809

[31]Yu J, Qi L, Jaroniec M. *J. Phys. Chem. C*, **2010**,**114**(30):13118-13125

[32]Galinska A, Walendziewski. *Energy Fuels*, **2005**,**19**(3):1143-1147

[33]Zhang M, Chen C, Ma W, et al. *Angew. Chem.*, **2008**,**120**(50):9876-9879

[34]Wang P, Wang J, Ming T, et al. *ACS Appl. Mater. Interfaces*, **2013**,**5**(8):2924-2929

[35]Lin W C, Yang W D, Huang I L, et al. *Energy Fuels*, **2009**,**23**(4):2192-2196

[36]Zhang C, Li Y, Wang Y, et al. *Environ. Sci. Technol.*, **2014**, **48**(10):5816-5822

[37]Nie L, Yu J, Li X, et al. *Environ. Sci. Technol.*, **2013**,**47**(6):2777-2783

[38]Huang H, Leung D Y. *ACS Catal.*, **2011**,**1**(4):348-354

[39]Bandara J, Udawatta C P K, Rajapakse C S K. *Photochem. Photobiol. Sci.*, **2005**,**4**(11):857-861

[40]Li G, Dimitrijevic N M, Chen L, et al. *J. Phys. Chem. C*, **2008**,**112**(48):19040-19044

[41]Montini T, Gombac V, Sordelli L, et al. *ChemCatChem*, **2011**, **3**(3):574-577

[42]Yu J, Ran J. *Energy Environ. Sci.*, **2011**,**4**(4):1364-1371

[43]Wu Y, Lu G, Li S. *Catal. Lett.*, **2009**,**133**(1/2):97-105

[44]Wu N L, Lee M S. *Int. J. Hydrogen Energy*, **2004**,**29**(15):1601-1605

[45]Chen X, Mao S S. *Chem. Rev.*, **2007**,**107**(7):2891-2959

[46]Fan J, Boettcher S W, Stucky G D. *Chem. Mater.*, **2006**,**18**(26):6391-6396

[47]Liu R, Ren Y, Shi Y, et al. *Chem. Mater.*, **2007**,**20**(3):1140-1146

[48]Hartmann P, Lee D K, Smarsly B M, et al. *ACS Nano*, **2010**,**4**(6):3147-3154

[49]Wu S H, Chen D H. *J. Colloid Interface Sci.*, **2004**,**273**(1):165-169

[50]Clausen B S, Grbk L, Steffensen G, et al. *Catal. Lett.*, **1993**, **20**(1/2):23-36

[51]Velu S, Suzuki K, Vijayaraj M, et al. *Appl. Catal. B*: *Environ.*, **2005**,**55**(4):287-299

[52]Van Ooij W. *Surf. Sci.*, **1977**,**68**:1-9

[53]Fang J, Bi X, Si D, et al. *Appl. Surf. Sci.*, **2007**,**253**(22):8952-8961

[54]Wang Y, Duan X, Zheng J, et al. *Catal. Sci. Technol.*, **2012**, **2**(8):1637-1639

[55]Xiong J, Wang Y, Xue Q J, et al. *Green Chem.*, **2011**,**13**:1-9

[56]Lisiecki I, Pileni M P. *J. Phys. Chem.*, **1995**,**99**(14):5077-5082

[57]Cason J P, Miller M E, Thompson J B, et al. *J. Phys. Chem. B*, **2001**,**105**(12):2297-2302

[58]Subramanian V, Wolf E E, Kamat P V. *J. Am. Chem. Soc.*, **2004**,**126**(15):4943-4950

[59]MurdochM, Waterhouse G I N, Nadeem M A, et al. *Nat. Chem.*, **2011**,**3**(6):489-492